metals

MDPI

Article

Erosive Wear Resistance Regarding Different Destabilization Heat Treatments of Austenite in High Chromium White Cast Iron, Alloyed with Mo

Alejandro Gonzalez-Pociño, Florentino Alvarez-Antolin * and Juan Asensio-Lozano

Materials Pro Group, Departamento de Ciencia de los Materiales e Ingeniería Metalúrgica, Universidad de Oviedo; Independencia 13, 33004 Oviedo, Spain; UO204622@uniovi.es (A.G.-P.); jasensio@uniovi.es (J.A.-L.)

* Correspondence: alvarezflorentino@uniovi.es; Tel.: +34-985-181-949

Received: 14 April 2019; Accepted: 5 May 2019; Published: 7 May 2019

Abstract: With the aim of improving erosive wear resistance in hypoeutectic white cast irons with 18% Cr and 2% Mo, several samples of this grade were subjected to different heat treatments at 1000 °C to destabilize the austenite. The dwell times at this temperature varied from 4 to 24 h and the samples were cooled in air or oil. The existing phases were identified and quantified by applying the Rietveld structural refinement method. The results were correlated with the hardness of the material and with the microhardness of the matrix constituent. The greatest resistance to erosive wear was achieved in those samples that had a higher percentage of secondary carbides. The longer the dwell time at the destabilization temperature of austenite, the greater the amount of precipitated secondary carbides. However, the percentage of dissolved eutectic carbides is also higher. These eutectic carbides were formed as a result of non-equilibrium solidification. Low cooling rates (in still air) can offset this solution of eutectic carbides via the additional precipitation of secondary carbides in the 600–400 °C temperature range. A sharp decrease is observed in the percentage of retained austenite in those treatments with dwell times at 1000 °C equal to or greater than 12 h, reaching minimum values of around 2% volume. The percentage of retained austenite was always lower after oil quenching and the hardness of oil quenched samples was observed to be greater than those quenched in air. In these samples, the maximum hardness value obtained was 993 HV after a 12 h dwell, which result from the optimum balance between the percentages of retained austenite and of precipitated carbides.

Keywords: high chromium white cast iron; Rietveld refinement; secondary carbides; X-ray diffraction; retained austenite

1. Introduction

White cast irons highly alloyed with Cr are used in environments where resistance to abrasive wear is a priority requirement. Up to approximately a 16% Cr content, the eutectic constituent is ledeburitic, where the matrix phase of this constituent is mixed carbides with a 3:1 stoichiometry. However, when the weight content of Cr exceeds 16%, the eutectic constituent is no longer ledeburitic but austenite, being the matrix phase of this eutectic, while the dispersed carbides that accompany it are mixed carbides with a 7:3 stoichiometry [1], presenting a similar morphology to bars or plates [2]. Due to the high concentration of dissolved elements in solid solution, the austenite displays high hardenability, so the precipitation of martensite is obtained by cooling in air [1]. As a result of the destabilization of austenite at temperatures around 1000 °C, Cr-rich secondary carbides precipitate [3–17] which promotes enhanced abrasion resistance and an increase in the Ms temperature [18], thereby leading to a reduction in retained austenite [19]. Previous studies confirm that the longer the dwell time at the aforementioned temperature, the greater the precipitation of these carbides [2]. Other studies indicate that a higher

fraction of secondary carbides could be obtained during tempering between 400 and 600 °C [20], with increasing percentages formed with higher severity quench media, for example, during cryogenic treatments [14,20,21]. The addition of Mo increases hardenability [6,22], increasing hardness [23], and enhancing wear resistance [24–26]. During high tempering processes, mixed $(Mo,X)_2C$ carbides, can nucleate heterogeneously at eutectic Cr rich carbide boundaries [10], progressing in the matrix [13]. The objectives of this paper were, on the one hand, to optimize the destabilization heat treatment of austenite and the type of quenching to increase wear resistance, and on the other, to correlate the results of hardness and wear with the microstructural variations resulting from these treatments. To this end, several samples were taken from a hypoeutectic white cast iron with 18% Cr and 2% Mo which was subjected to several destabilization heat treatments at 1000 °C, employing different dwell times ranging from 4 to 24 h and subsequent cooling in air or oil. The aim of testing several dwell times at 1000 °C was to assess the possible impoverishment in chromium and carbon of the austenite, which would lead to an increase in the Ms temperature. This increase would reduce the theoretical risk of cracking on quenching, allowing this cooling to take place in oil and producing a decrease in the retained austenite.

2. Materials and Methods

Table 1 shows the chemical composition of the white cast iron under analysis. Prior to preparing the samples, the as-cast material was subjected to an isothermal treatment at 700 °C for 24 h with air cooling to facilitate the cutting of the samples. This treatment was reported to increase hardness after subsequent quench [27]. In all, 8 samples were treated at 1000 °C for 4, 8, 12, and 24 h in pairs and then quenched in air or oil. The evolution of the material's microstructure following these heat treatments was analyzed by means of optical microscopy (Nikon, Tokyo, Japan) and scanning electron microscopy (JEOL, Nieuw-Vennep, The Netherlands). Grinding was carried out with 60, 120, 240, 400, and 600 grit size SiC paper. Subsequently, the samples were polished in two consecutive stages with 6 μm and 1 μm diamond paste, respectively. Nital 5 was used as the chemical reagent to reveal the microstructure of the material. The percentages and types of precipitated phases were determined by X-ray diffraction, employing molybdenum as the emitting metal. The diffractograms were measured on the Seifert XRD 3000 T/T diffractometer (Baker Hughes, Celle, Germany) employing a Bragg-Brentano parfocal optical configuration with reverse rotation coupled to the detector. The radiation emitted by the fine focus Mo tube, at 40 kV and 40 mA, was monochromatized to the Kα doublet: λ_1 = 0.709316 Å and λ_2 = 0.713607 Å. The patterns were recorded by means of a NaI (Tl) scintillation detector measuring the 2θ angular range. This was found to be between 12° and 56°, with a 0.025° step and a counting time per step of 30 s. Determination of the percentage of crystalline phases was established by fitting the aforementioned diffractograms using the Rietveld structural refinement method. To do so, starting with the recording of the diffraction figures obtained in both grades, a structural refinement was carried out using the crystallographic information files present in the ICSD inorganic structures database (version 2016, FIZ Karlsruhe, Eggenstein-Leopoldshafen, Germany) belonging to the phases that, according to the technical literature, may be precipitated after the various thermal treatments. These mainly include: Martensite (α'), Austenite (γ), mixed Cr/Fe carbides (in particular with 3:2, 7:3 and 23:6 stoichiometries) and mixed Mo_2C and Fe_3C carbides [1,28,29]. Applying the Rietveld structural refinement method, a fitting of the diffraction experimental figures was consequently made based on the diffraction patterns of these phases.

To measure the overall hardness of each sample, the Vickers hardness was measured applying a 10 N load. Furthermore, the hardness of the eutectic constituent, without including primary carbides, was obtained applying a 0.5 N load. In all cases, 10 indentations were made in each of the samples. The diagonals of the indentations were measured under an optical microscope at 1000 magnifications.

The erosive wear resistance was measured by means of compressed air blasting with corundum particles according to the ASTM G76 standard, applying a pressure of 4 bar, a flow rate of 160 g/min and a 30° angle of incidence on the sample surface. Five repetitions were performed for each experimental

condition. The duration of each test was set to 1 min. The dimensions of the experimental specimens corresponded to prisms of 50 by 30 by 10 mm^3.

Table 1. Chemical composition of the analyzed samples (wt. %).

C	Si	Mn	Cr	Mo	S	P
3.0	1.2	0.8	18.2	2.0	0.009	0.024

3. Results

Figure 1 shows the microstructure obtained in the as-cast state. The presence of eutectic carbides and pearlite can be observed in a matrix with abundant retained austenite. A high percentage of the eutectic constituent and a relatively fine structure of this constituent are observed. This suggests the possibility of non-equilibrium solidification. By means of an isothermal treatment at 700 °C, the retained austenite may be transformed into pearlite, thereby favoring subsequent machining for the preparation of the samples (Figure 2).

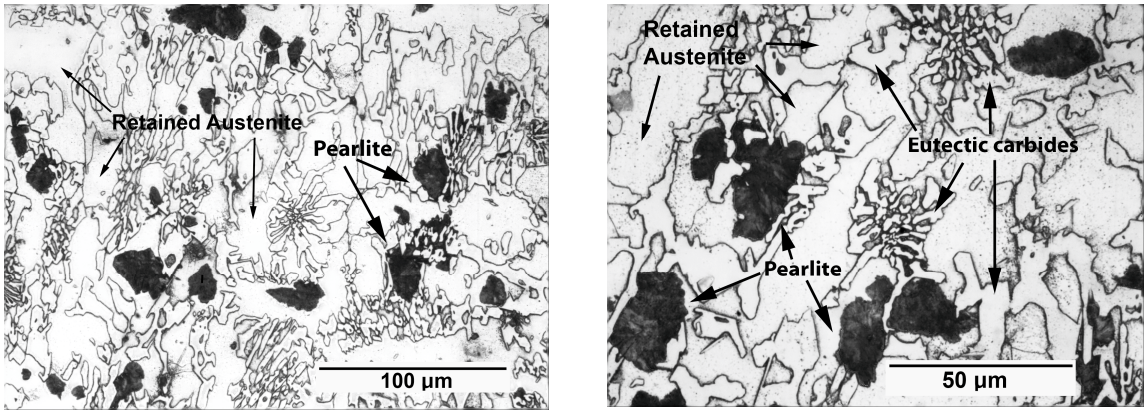

(**a**) (**b**)

Figure 1. Microstructure obtained in the as-cast state. Optical microscope: (**a**) 500 magnifications; (**b**) 1000 magnifications.

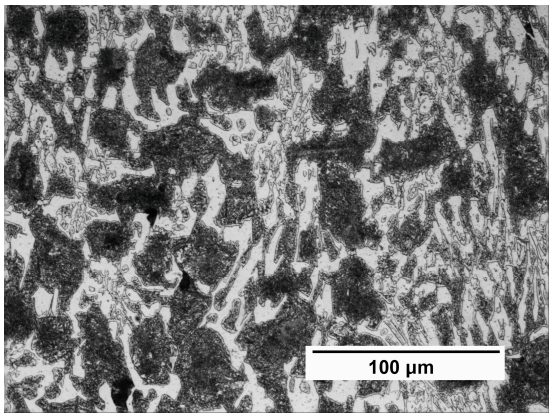

Figure 2. Microstructure after an isothermal treatment at 700 °C for 24 h. Optical microscope: 500 magnifications.

Figure 3 shows the microstructure obtained after the different heat treatments at 1000 °C used to destabilize the austenite. The microstructure is made up of proeutectic austenite and a eutectic constituent in which austenite forms the matrix phase, while the dispersed phase is formed by eutectic M_7C_3 carbides. This austenite would have been mainly transformed into martensite. The presence of

secondary carbides largely precipitated in the proeutectic austenite and showing a darker coloring than the austenite of the eutectic constituent, is worth noting. The greater density of secondary carbides in the proeutectic austenite compared to the austenite of the eutectic constituent may be due to the segregation of Mo towards the eutectic liquid, favoring the enrichment of the eutectic austenite in this element, which has an inhibiting effect on the precipitation of secondary carbides [30]. The observed microstructure is a consequence of three simultaneously competing kinetics:

1. A greater density of secondary carbides with increasing dwell time at 1000 °C, which leads to an increase in the Ms temperature, thus favoring a decrease in the retained austenite.
2. Also, as the dwell time at 1000 °C is increased, the dissolution of those eutectic carbides that have precipitated as a consequence of the non-equilibrium solidification takes place.
3. Furthermore, additional precipitation of secondary carbides takes place in the 600–400 °C temperature range when the cooling rate is low (cooling in still air).

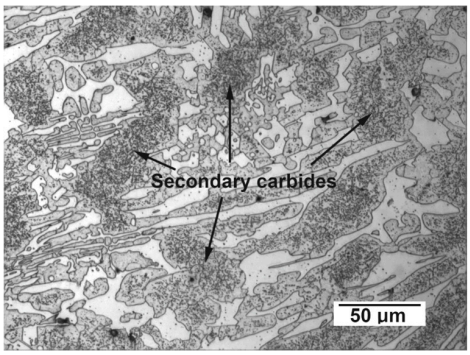

(**a**) After 4 h dwell time at 1000 °C and air quenching

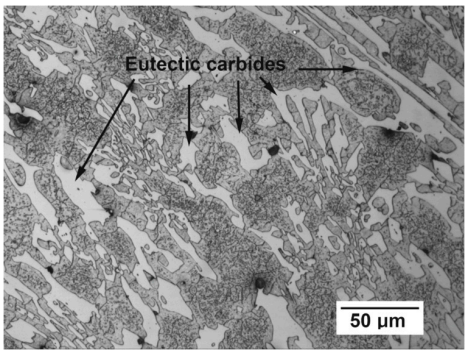

(**b**) After 8 h dwell time at 1000 °C and air quenching

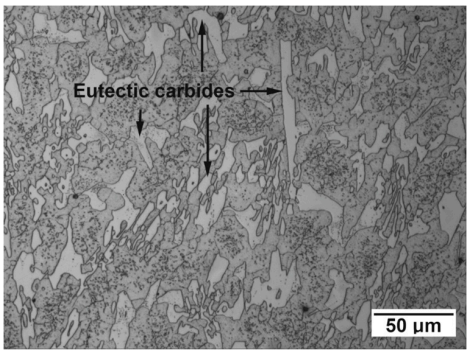

(**c**) After 12 h dwell time at 1000 °C and air quenching

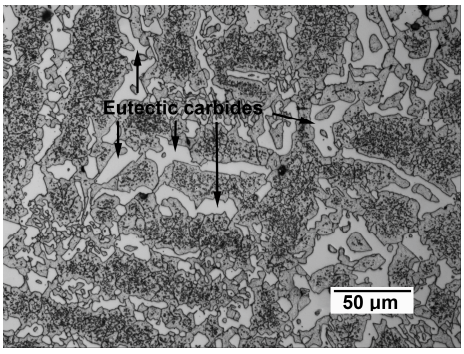

(**d**) After 24 h dwell time at 1000 °C and air quenching

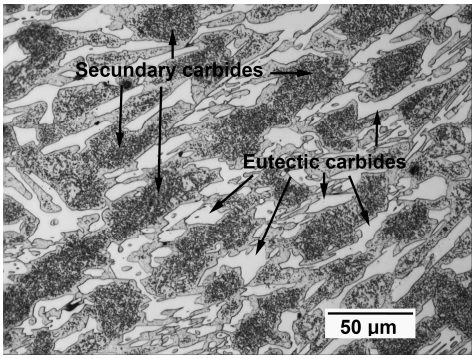

(**e**) After 4 h dwell time at 1000 °C and oil quenching

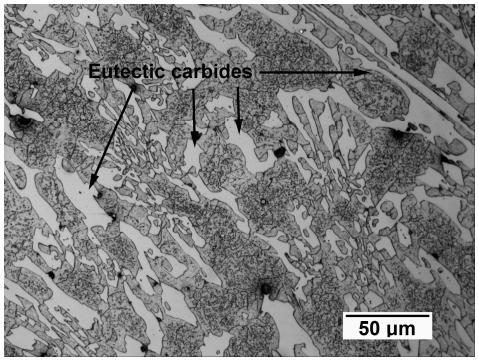

(**f**) After 8 h dwell time at 1000 °C and oil quenching

Figure 3. *Cont.*

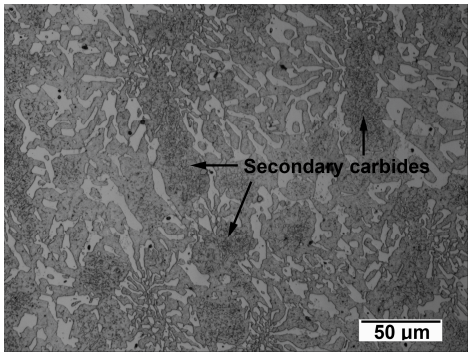

(**g**) After 12 h dwell time at 1000 °C and oil quenching

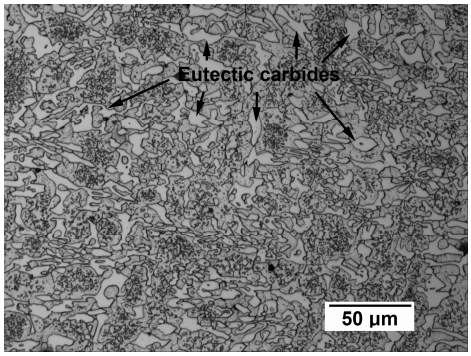

(**h**) After 24 h dwell time at 1000 °C and oil quenching

Figure 3. Microstructure after the different treatments for destabilizing the austenite. Optical microscope: 500 magnifications.

Figure 4 shows the diffractograms obtained after the different heat treatments used to destabilize the austenite. Figure 4a represents the air-quenched samples and Figure 4b, the oil-quenched samples. The Rietveld structural refinement method was used to identify the existing phases and determine their weight percentages.

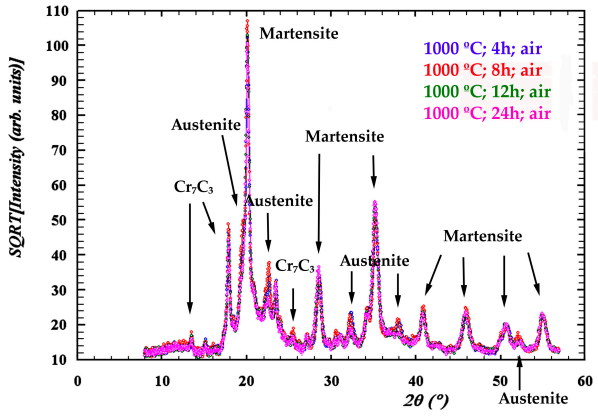

(**a**)

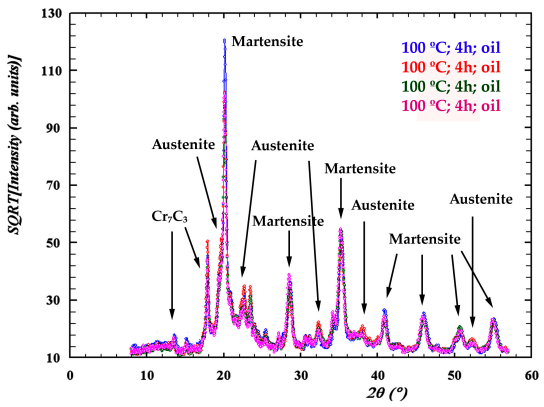

(**b**)

Figure 4. (**a**) Diffractograms for the air-quenched samples; (**b**) diffractograms for the oil-quenched samples.

Table 2 shows the volume percentages of the identified phases in each diffractogram. The percentage of retained austenite is always seen to be lower in the oil-quenched samples. In general, an abrupt decrease in the percentage of retained austenite is observed in the destabilization treatments with a dwell time of 12 and 24 h compared to those lasting 4 and 8 h. On the other hand, it can be seen that the precipitated carbides are all of the M_7C_3 type. The specimens cooled in air showed a smaller difference between the percentages by volume of total carbides, ranging between 52% and 55%. However, these variations were found to be greater in the samples quenched in oil, whose values were comprised between 43% to 56%. In both cases, the overall percentage of carbides is a consequence of the following:

- The longer the dwell time at 1000 °C, the greater the percentage of precipitated secondary carbides.
- The longer the dwell time at 1000 °C, the greater the percentage of eutectic carbides that dissolve. These eutectic carbides will be those formed as a result of non-equilibrium solidification. It should be noted that the solubility limit of the C in the austenite will increase until 1000 °C is reached.

- Moreover, additional precipitation of secondary carbides in the 600–400 °C temperature range is produced in air-cooled samples. This precipitation tends to offset the dissolution of eutectic carbides.

In the oil-quenched samples, the lowest percentage of total carbides is obtained in the samples with the shortest and longest dwell times at the destabilization temperature, i.e., 4 and 24 h, respectively. Four hours at 1000 °C is not enough time for a significant number of secondary carbides to precipitate. After 24 h at 1000 °C, the dissolution of eutectic carbides has offset the precipitation of secondary carbides. The highest percentage of carbides is obtained after 8 h dwell time at 1000 °C, subsequently decreasing slightly after a dwell time of 12 h and once again reaching the minimum percentage of carbides after a dwell time of 24 h. The comparison between the samples with a 4 h dwell time at 1000 °C and respective cooling in air and oil is worth highlighting. The samples that were cooled in air reach 55.17% by volume of carbides; however, those cooled in oil only reach 43.33%. The slower cooling equivalent to a staircase where horizontal sections are longer than if the cooling was faster. This would favor the precipitation of new secondary carbides in the temperature range between 600 and 400 °C.

Table 2. Microstructural parameters and weight distributions of the precipitated phases. Esd represents the statistical error.

Quenching (Destabilization Heat Treatment at 1000 °C)		Rietveld Fitting	Phases	Bragg R-Factor	Volume %	Esd.
Air	4 h	R_{wp} = 9.66 Chi^2 = 2.37	α′ γ M_7C_3	1.5 4.76 2.72	36.59 8.24 55.17	±094 ±0.41 ±1.51
	8 h	R_{wp} = 11 Chi^2 = 2.77	α′ γ M_7C_3	1.04 7.86 4.5	35.48 9.94 54.58	±0.91 ±0.44 ±1.47
	12 h	R_{wp} = 10.2 Chi^2 = 2.62	α′ γ M_7C_3	4.39 5.54 3.71	45.63 2.61 51.76	±1.07 ±0.29 ±1.50
	24 h	R_{wp} = 10.7 Chi^2 = 2.74	α′ γ M_7C_3	5.34 6.15 4.58	44.30 2.83 52.87	±1.1 ±0.3 ±1.54
Oil	4 h	R_{wp} = 11.3 Chi^2 = 2.77	α′ γ M_7C_3	3.96 8.28 8.82	50.09 6.59 43.33	±1.49 ±0.42 ±1.63
	8 h	R_{wp} = 10.9 Chi^2 = 1.99	α′ γ M_7C_3	3.43 3.85 4.69	36.53 6.94 56.52	±1.17 ±0.57 ±1.80
	12 h	R_{wp} = 11.7 Chi^2 = 2.67	α′ γ M_7C_3	8.16 8.9 8.12	44.84 2.26 52.90	±1.39 ±0.45 ±1.84
	24 h	R_{wp} = 11.6 Chi^2 = 2.45	α′ γ M_7C_3	6.44 9.1 8.47	51.35 2.22 46.43	±1.57 ±0.48 ±1.81

Figure 5 shows a representative image of both cases, where it can be seen that the density and size of secondary carbides is significantly lower when the cooling takes place in oil.

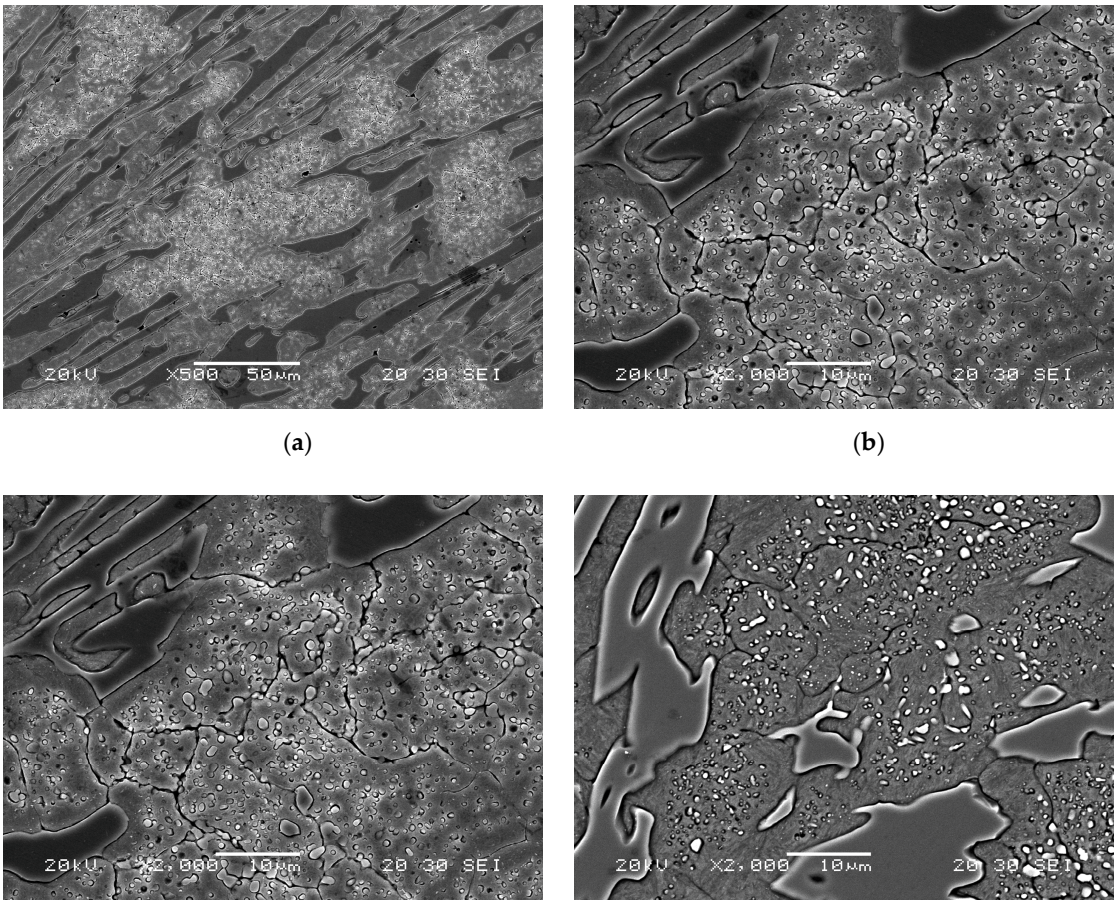

(**a**) (**b**)

(**c**) (**d**)

Figure 5. Comparison of the density of secondary carbides in samples subjected to destabilization heat treatments of 4 h and quenching in air or oil. Scanning electron microscope; (**a**) quenching in air. 500×; (**b**) quenching in air. 2000×; (**c**) quenching in oil. 500×; (**d**) quenching in oil. 2000×.

Figure 6 shows the hardness values obtained. Figure 6a shows the hardness of the material applying a 10 N load. Note that the hardness is always higher after oil quenching. In air quenching, the hardness is also found to increase with increasing dwell time at the destabilization temperature, while the retained austenite decreases. However, among the samples quenched in oil, the highest hardness was obtained when the destabilization heat treatment lasted 12 h, in which a very low amount of retained austenite (2.26%) and a high amount of carbides (52.90%) were obtained. Figure 6b shows the microhardness values obtained in the matrix constituent applying a 0.5 N load. In this case, the highest hardness among the samples quenched in oil is once again obtained after 12 h dwell time at 1000 °C, which is when the optimum balance between retained austenite and secondary carbides is reached. When the dwell time is 24 h, there is a decrease in the total percentage of carbides (to 46.43%). In the case of the air-quenched samples, in which the percentage of carbides under goes a much lower variation than in those quenched in oil, the highest hardness of the matrix constituent is obtained in the sample subjected to the destabilization heat treatment at 1000 °C for 24 h, resulting in a lower percentage of retained austenite.

Figure 7 shows the results obtained after the wear test. The error bar shows the difference between the average value and the maximum and minimum values reached.

In the case of the specimens that were cooled in the air, the highest wear resistance is obtained after 4 and 24 h of dwell at the destabilizing temperature, which correspond to the samples with a higher percentage by weight of carbides. And yet the treatment of 4 h at 1000 °C provided the lowest hardness value. This is thought to be related to the high presence of retained austenite leading to

a somewhat lower hardness, and the higher fraction of secondary carbides conducting to a better performance in the erosive wear testing in turn. In contrast to this, the sample that remained 24 h at 1000 °C displayed the highest hardness, and the lowest austenite retained.

In the case of the specimens that were oil quenched, a maximum in the wear resistance were obtained after 8 and 12 h of austenite destabilization, which corresponds to the samples for which the highest percentage of secondary carbides were measured. Out of these, the sample which was subjected to a 12 h destabilization treatment and checked to have a higher hardness had a lower percentage of retained austenite in its microstructure. It then follows that an optimal resistance to erosive wear could be achieved with the highest percentage of secondary carbides formed during the destabilization of austenite. And it seems less relevant for improved wear resistance the resulting hardness achieved by martensite, carbides, and retained austenite [11,13,17]. In turn, the percentage of secondary carbides formed over destabilization period seems to be influenced, not only by the dwell time at the destabilization temperature, but also by the cooling rate.

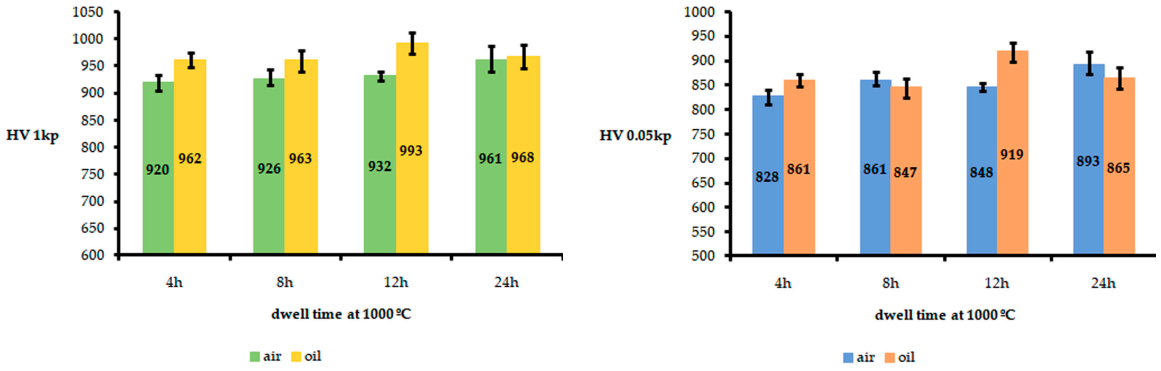

(**a**) (**b**)

Figure 6. Hardness values. The error bars show the distance between the mean value and the maximum and minimum values. Ten (10) indentations were made in each sample; (**a**) hardness values obtained in the overall microstructure applying a 10 N load; (**b**) hardness values obtained in the constituent matrix applying a 0.5 N load.

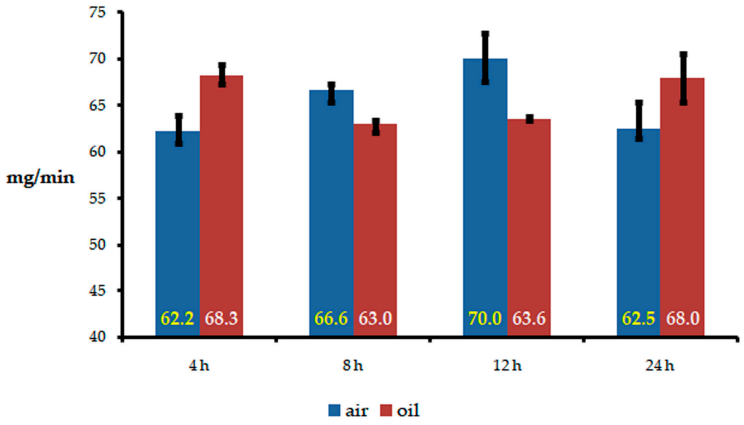

Figure 7. Resistance to erosive wear. Weight loss per unit of time.

4. Conclusions

After performing different heat treatments at 1000 °C to destabilize the austenite in white cast irons with 18% Cr and 2% Mo, with quenching in air and oil, the following conclusions may be drawn:

1. The longer the dwell time at the destabilization temperature of austenite (1000 °C), the greater the amount of precipitated secondary carbides. However, the percentage of dissolved eutectic carbides is also higher. These dissolved eutectic carbides will have been formed as a result of non-equilibrium solidification. Low cooling rates (in still air) can offset this solution of carbides via the additional precipitation of secondary carbides in the 600–400 °C temperature range.
2. The erosive wear resistance depends mainly on the volume fraction of secondary carbides precipitated during the destabilization of austenite. The maximum wear resistance in air cooled samples corresponded to a destabilizing treatment at 1000 °C for 4h and 24 h. However, in those samples quenched in oil, the maximum wear resistances were obtained on those samples destabilized at 1000 °C for 8 h and 12 h.
3. There is a sharp decrease exists in the percentage of retained austenite in those treatments with dwell times at 1000 °C equal to or greater than 12 h, reaching minimum values of around 3 wt. %.
4. In the oil-quenched samples, the lowest percentage of carbides obtained is 43–46% after dwell times of 4 h and 24 h, reaching a maximum value of 56% when employing a dwell time of 8 h.
5. In the air-quenched samples, an increase in hardness is observed with increasing dwell time at the destabilization temperature and as the retained austenite decreases, obtaining a maximum hardness of 961 HV after a dwell time of 24 h. In the oil-quenched samples, however, the maximum hardness was 993 HV after a dwell time of 12 h, which is when an optimum balance is obtained between the percentages of retained austenite and the percentages of precipitated carbides.

Author Contributions: J.A.-L. conceived and designed the investigation; A.G.-P. performed all laboratory work; F.A.-A. led the investigation, analyzed the data and wrote the paper.

Funding: This research received no external funding

Conflicts of Interest: The authors declare no conflict of interest.

References

1. Pero-Sanz, J.A. *Fundiciones Férreas*; Dossat: Madrid, Spain, 1994; p. 154.
2. Bedolla-Jacuinde, A.; Arias, L.; Hernandez, B. Kinetics of secondary carbides precipitation in a high-chromium white iron. *J. Mater. Eng. Perform.* **2003**, *12*, 371–382. [CrossRef]
3. Powell, G.L.F.; Bee, J.V. Secondary carbide precipitation in an 18 wt.% Cr-1 wt.% Mo white iron. *J. Mater. Sci.* **1996**, *31*, 707–711. [CrossRef]
4. Zhi, X.H.; Xing, J.D.; Gao, Y.M.; Fu, H.G.; Peng, J.Y.; Xiao, B. Effect of heat treatment on microstructure and mechanical properties of a Ti-bearing hypereutectic high chromium white cast iron. *Mater. Sci. Eng. A* **2008**, *487*, 171–179. [CrossRef]
5. Carpenter, S.D.; Carpenter, D.; Pearce, J.T.H. XRD and electron microscope study of a heat treated 26.6% chromium white iron microstructure. *Mater. Chem. Phys.* **2007**, *101*, 49–55. [CrossRef]
6. Karantzalis, A.E.; Lekatou, A.; Diavati, E. Effect of Destabilization Heat Treatments on the Microstructure of High-Chromium Cast Iron: A Microscopy Examination Approach. *J. Mater. Eng. Perform.* **2009**, *18*, 1078–1085. [CrossRef]
7. Kootsookos, A.; Gates, J.D. The role of secondary carbide precipitation on the fracture toughness of a reduced carbon white iron. *Mater. Sci. Eng. A* **2008**, *490*, 313–318. [CrossRef]
8. Efremenko, V.; Shimizu, K.; Chabak, Y. Effect of Destabilizing Heat Treatment on Solid-State Phase Transformation in High-Chromium Cast Irons. *Metall. Mater. Trans. A* **2013**, *44*, 5434–5446. [CrossRef]
9. Liu, Q.; Shibata, H.; Hedstrom, P.; Joonsson, P.G.; Nakajima, K. Dynamic Precipitation Behavior of Secondary M7C3 Carbides in Ti-alloyed High Chromium Cast Iron. *Isij Int.* **2013**, *53*, 1237–1244. [CrossRef]
10. Wiengmoon, A.; Pearce, J.T.H.; Chairuangsri, T. Relationship between microstructure, hardness and corrosion resistance in 20 wt. % Cr, 27 wt. % Cr and 36 wt. % Cr high chromium cast irons. *Mater. Chem. Phys.* **2011**, *125*, 739–748. [CrossRef]
11. Bedolla-Jacuinde, A.; Guerra, F.V.; Mejia, I.; Zuno-Silva, J.; Rainforth, M. Abrasive wear of V-Nb-Ti alloyed high-chromium white irons. *Wear* **2015**, *332*, 1006–1011. [CrossRef]

12. Lai, J.P.; Pan, Q.L.; Sun, Y.W.; Xiao, C.A. Effect of Si Content on the Microstructure and Wear Resistance of High Chromium Cast Iron. *ISIJ Int.* **2018**, *58*, 1532–1537. [CrossRef]
13. Antolin, J.F.A.; Garrote, L.F.; Lozano, J.A. Application of Rietveld Refinement to the correlation of the microstructure evolution of white cast irons with 18 and 25%-wt. Cr after oil quench and successive temper treatments, with abrasive wear and bending testing. *Rev. Metal.* **2018**, *54*, 11. [CrossRef]
14. Wang, J.; Xiong, J.; Fan, H.Y.; Yang, H.S.; Liu, H.H.; Shen, B.L. Effects of high temperature and cryogenic treatment on the microstructure and abrasion resistance of a high chromium cast iron. *J. Mater. Process. Technol.* **2009**, *209*, 3236–3240. [CrossRef]
15. Liu, H.H.; Wang, J.; Yang, H.S.; Shen, B.L. Effects of cryogenic treatment on microstructure and abrasion resistance of CrMnB high-chromium cast iron subjected to sub-critical treatment. *Mater. Sci. Eng. A* **2008**, *478*, 324–328. [CrossRef]
16. Filipovic, M.M. Iron-chromium-carbon-vanadium white cast irons—The microstructure and properties. *Hemijska Industrija* **2014**, *68*, 413–427. [CrossRef]
17. Guitar, M.A.; Suarez, S.; Prat, O.; Guigou, M.D.; Gari, V.; Pereira, G.; Mucklich, F. High Chromium Cast Irons: Destabilized-Subcritical Secondary Carbide Precipitation and Its Effect on Hardness and Wear Properties. *J. Mater. Eng. Perform.* **2018**, *27*, 3877–3885. [CrossRef]
18. Jia, X.S.; Hao, Q.G.; Zuo, X.W.; Chen, N.L.; Rong, Y.H. High hardness and toughness of white cast iron: The proposal of a novel process. *Mater. Sci. Eng. A* **2014**, *618*, 96–103. [CrossRef]
19. Gasan, H.; Erturk, F. Effects of a Destabilization Heat Treatment on the Microstructure and Abrasive Wear Behavior of High-Chromium White Cast Iron Investigated Using Different Characterization Techniques. *Metall. Mater. Trans. A* **2013**, *44*, 4993–5005. [CrossRef]
20. Liu, H.H.; Wang, J.; Shen, B.L.; Yang, H.S.; Gao, S.J.; Huang, S.J. Effects of deep cryogenic treatment on property of 3Cr13Mo1V1.5 high chromium cast iron. *Mater. Des.* **2007**, *28*, 1059–1064. [CrossRef]
21. Yang, H.S.; Wang, J.; Shen, B.L.; Liu, H.H.; Gao, S.J.; Huang, S.J. Effect of cryogenic treatment on the matrix structure and abrasion resistance of white cast iron subjected to destabilization treatment. *Wear* **2006**, *261*, 1150–1154. [CrossRef]
22. Inthidech, S.; Sricharoenchai, P.; Matsubara, Y. Effect of molybdenum content on subcritical heat treatment behaviour of hypoeutectic 16 and 26 wt-% chromium cast irons. *Int. J. Cast Met. Res.* **2012**, *25*, 257–263. [CrossRef]
23. Cetinkaya, C. An investigation of the wear behaviours of white cast irons under different compositions. *Mater. Des.* **2006**, *27*, 437–445. [CrossRef]
24. Li, Y.C.; Li, P.; Wang, K.; Li, H.Z.; Gong, M.Y.; Tong, W.P. Microstructure and mechanical properties of a Mo alloyed high chromium cast iron after different heat treatments. *Vacuum* **2018**, *156*, 59–67. [CrossRef]
25. Oh, H.; Lee, S.; Jung, J.Y.; Ahn, S. Correlation of microstructure with the wear resistance and fracture toughness of duocast materials composed of high-chromium white cast iron and low-chromium steel. *Metall. Mater. Trans. A* **2001**, *32*, 515–524. [CrossRef]
26. Scandian, C.; Boher, C.; de Mello, J.D.B.; Rezai-Aria, F. Effect of molybdenum and chromium contents in sliding wear of high-chromium white cast iron: The relationship between microstructure and wear. *Wear* **2009**, *267*, 401–408. [CrossRef]
27. Wiengmoon, A.; Khantee, J.; Pearce, J.T.H.; Chairuangsri, T. Effect of pre-annealing heat treatment on destabilization behavior of 28 wt. % Cr-2.6 wt. % C high-chromium cast iron. In Proceedings of the 7th Global Conference on Materials Science and Engineering (CMSE2018), Xi'an, China, 1–4 November 2018.
28. Fairhust, W.; Rohrig, K. Abrasion resistant high chromium cast irons. *Foundry Trade J.* **1974**, *136*, 685–698.
29. Wang, J.; Li, C.; Liu, H.H.; Yang, H.S.; Shen, B.L.; Gao, S.J.; Huang, S.J. The precipitation and transformation of secondary carbides in a high chromium cast iron. *Mater. Charact.* **2006**, *56*, 73–78. [CrossRef]
30. Efremenko, V.G.; Chabak, Y.G.; Brykov, M.N. Kinetic Parameters of Secondary Carbide Precipitation in High-Cr White Iron Alloyed by Mn-Ni-Mo-V Complex. *J. Mater. Eng. Perform.* **2013**, *22*, 1378–1385. [CrossRef]